MODELING OF MACROSEGREGATION IN ELECTROSLAG REMELTING OF SUPERALLOYS

C. L. Jeanfils, J. H. Chen, H. J. Klein
STELLITE DIVISION, Cabot Corporation, Kokomo, Indiana

The present status of a mathematical simulation of the electroslag remelting process is reviewed. The model is used to calculate the transient temperature field in an ESR ingot and to calculate the extent of macrosegregation that arises in a multicomponent alloy that solidifies into a single solid phase.

INTRODUCTION

The objective of this work is to develop a model by which the limitations in melt rate and ingot size can be calculated for the remelting of a particular alloy in ESR. For a given ingot size, there is a melt rate above which unacceptable segregation and at times, freckles, occur. This limiting melt rate varies according to the alloy grade and the practice (slag cap height, electrode depth of immersion, fill ratio).

The approach taken has been to model, one at a time, several aspects of the ESR process due to its complex nature. The other aspects are treated, temporarily, as boundary or imposed conditions. For example, in the heat transfer analysis, it was assumed that the melt rate and the slag temperature are known functions of time. A more rigorous treatment would be to solve the energy and momentum transport equations in the slag and liquid metal pool, such as presented in References 1 and 2.

Two aspects of the modeling of the ESR process will be described here. One is concerned with changes in pool characteristics during transients in melt rate; these changes are believed to be a major cause of ingot defects. The other aspect is concerned with the flow of interdendritic liquid in

the mushy zone. This flow, if extensive, results in macrosegregation and, at times, in freckles. This macrosegregation theory was developed by M. C. Flemings, R. Mehrabian, and their coworkers at MIT in the 60's (3-6). The modeling of the temperature field in ingots produced by electrode remelting was reviewed recently by Ballantyne and Mitchell (7).

The heat transfer analysis provides the necessary inputs to the macrosegregation analysis, such as liquidus and solidus isotherm shapes and velocities.

MATHEMATICAL MODELS

Heat Transfer in the Ingot

The approach employed was presented in a recent paper by Jeanfils et al, and only a brief discussion of the methodology will thus be given here (8).

For a cylindrical ingot, the basic equation to be solved is:

$$\frac{\partial H}{\partial t} = \nabla(k\nabla T) + v\frac{\partial H}{\partial z} \qquad (1)$$

where,

H = the enthalpy per unit volume
t = time
k = thermal conductivity
T = temperature

The velocity v is that of the frame of reference in which Equation 1 is solved with respect to the frame of reference in which the conductive heat flux q is described by:

$$q = -k\nabla T \qquad (2)$$

Two natural frames of reference are one, fixed in the ingot, the other, moving with the slag metal interface. For constant solid density, the velocity v vanishes in the first frame, while at steady state, the left hand side of Equation 1 vanishes in the second frame for the upper portion of the ingot.

The convective transport of heat by liquid motion with respect to the ingot is neglected.

In Reference 8, it was shown that the steady state for the pool shape of the higher temperature isotherms was reached after the ingot height had reached about one and a half diameters. Steady state is never really reached for the temperature field in the lower portion of the ingot.

The enthalpy term contains the specific heat and the latent heat of fusion. A typical rate of change of the enthalpy with temperature for the solidification range is shown in Figure 1a.

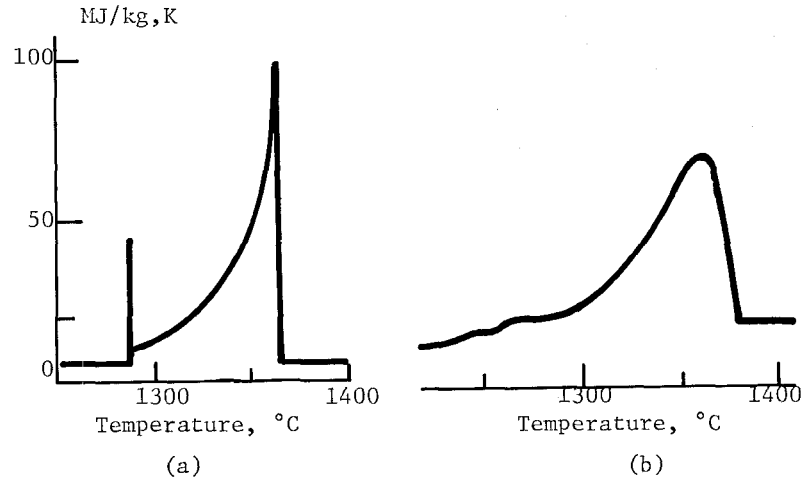

Figure 1: Calculated effective heat capacity per unit volume. (a) Experimental DTA Cooling Curve, (b) for Waspaloy.

This rate of change, an effective heat capacity per unit volume, was calculated for Waspaloy under the following conditions: (1) the total latent heat equals 256 kJ/kg (110 BTU/lb.), (2) only one solid phase forms, and (3) partition ratios for the solutes are constant. For comparison, a cooling DTA curve is shown for this alloy in Figure 1b.

The alternating direction implicit method is used to solve Equation 1, subject to appropriate boundary conditions.

Macrosegregation

The equations describing macrosegregation caused by interdendritic fluid flow in ESR ingots have been presented in a recent paper for the case of a binary alloy with a steady pool shape (9). Fujii et al treat the case of fluid flow in the mushy zone of a multicomponent low alloy steel ingot growing horizontally (10). These references and the original articles on the subject should be consulted for the derivation of the equations (3-6). Briefly, the assumptions of constant solid density and of equilibrium of composition at the liquid-solid interface are made. Differential volume elements are considered; integration over these elementary volumes is used to define local quantities such as volume fraction liquid and liquid composition. These local quantities are treated as continuous variables that can be differentiated. The conservation of total mass and of solutes is then expressed mathematically. The equation of motion for the liquid is replaced by Darcy's Law; the latter relates the fluid velocity to the gradient of pressure and to body forces such as gravity. By combining these equations, one arrives at a set of partial differential equations where the dependent variables are scalars: the local pressure, the local volume fraction liquid, and the temperature. These equations are often uncoupled and the temperature problem is treated separately from the fluid flow and volume fraction liquid calculation. This was the approach taken in this paper, however, work is currently underway to treat the coupled problem for the ESR case. The treatment of a coupled problem is given in detail by Fujii et al (10).

For a multicomponent system, the solidification path must be calculated if it is not known independently. If only one solid phase is forming, and if Equations 1 and 2 designate two solutes which do not diffuse substantially in the solid, then (11):

$$\frac{D \ln C_{L2}}{D \ln C_{L1}} = \frac{1 - k_2}{1 - k_1} \qquad (3)$$

where,

D = the differential following the fluid motion

C_{L1} = the weight fraction of the component 1

k_1 = the partition ratio for the component 1 (the weight fraction in the solid divided by the weight fraction in the liquid)

If C_{L1} is considered to be the independent variable, and the initial concentrations are known, Equation 3 can be integrated, provided the ratio on the right hand side of Equation 3 is known.

On the other hand, if 1 designates a solute that does not diffuse substantially in the solid, while 2 represents a solute that diffuses readily, one obtains (3,10):

$$\frac{D \ln C_{L1}}{Dt} = -(1 - k_1) \frac{\rho_s}{\rho_L} \frac{1}{g_L} \frac{\partial g_L}{\partial t} \tag{4a}$$

$$\frac{D \ln C_{L2}}{Dt} = -(1 - k_2) \frac{\rho_s}{\rho_s k_2 (1 - g_L) + \rho_L g_L} \frac{\partial g_L}{\partial t} \tag{4b}$$

where,

$\frac{D}{Dt} = \frac{\partial}{\partial t} + W \cdot \nabla$ is the substantive derivative

w = the velocity of the fluid

ρ_s, ρ_L = the density of the solid and of the liquid

g_L = the volume fraction of the liquid

Dividing Equation 4b by Equation 4a, one obtains:

$$\frac{D \ln C_{L2}}{D \ln C_{L1}} = \frac{(1 - k_2)}{(1 - k_1)} \frac{\rho_L g_L}{[\rho_L g_L + (1 - k_L) \rho_s k_2]} \tag{5}$$

For modeling the solidification of a Waspaloy ingot, titanium is taken as element 1. Equation 3 is integrated for the solutes aluminum, molybdenum, cobalt, and chromium. Equation 5 is used for carbon and is integrated numerically, since the volume fraction of liquid and the liquid density are part of the integrand.

Expressions relating the temperature to the liquid compo-

sition and the liquid density to the composition and temperature are also required. The solid and liquid densities were calculated using literature data and assuming that the specific volume of the alloy is the weighted sum of the specific volumes of its constituents (12,13,14). However, for the alloying elements that do not solidify to form a close packed structure, the specific volume of that element in a solid nickel-based superalloy was taken to be 5% lower than its specific volume in the liquid. Due to the lack of data for carbon, it was assumed that it had the same specific volume in the solid and in the liquid.

For a dilute multicomponent alloy, the dependence of the liquidus temperature on the solute concentration is deduced from binary phase diagrams (10,15). To determine whether this approach was applicable to a non-dilute superalloy, in this case Waspaloy, the liquidus of several alloys of enriched solute content was measured by DTA. Eight samples were run and the range of composition covered was: Ti, 3 to 4.5%; Al, 1.3 to 3%; Mo, 4.3 to 7.6%; Cr, 19 to 22.4%; C, 0.09 to 0.14%. The following equation predicts the liquidus of the eight samples to within 1°C.

$$T_L\ (°C) = 1364 - 15.2\ (\%\ Ti - 3.00) + 0.4\ (\%\ Co - 13.50) - 9.4\ (\%\ Al - 1.50) - 2.8\ (\%\ Cr - 19.50) - 4.6\ (\%\ Mo - 4.30) - 104\ (\%\ C - 0.08) \quad (6)$$

The coefficient for cobalt was estimated from the binary cobalt-nickel diagram. When these coefficients in Equation 6 are compared to those predicted by the binary phase diagrams, it is seen that for a given solute these coefficients are of the same order of magnitude, but that the effect determined experimentally is consistently stronger. The coefficient for carbon should be viewed with caution since the composition range covered experimentally is narrow.

Table 1. COMPARISON OF THE AVERAGE COMPOSITION OF A "WASPALOY" FRECKLE WITH THE COMPOSITION ADJACENT TO THE FRECKLE.

	Freckle	Outside Freckle	Ratio
Titanium	4.51%	2.80%	1.61
Molybdenum	5.01%	4.09%	1.23
Aluminum	1.78%	1.57%	1.13
Cobalt	12.82%	13.86%	0.93
Chromium	18.98%	18.89%	1.01
Nickel	56.89%	58.78%	0.97

The ingot growth rate corresponding to the first variation in melt rate is shown in Figure 2. In order to determine if chemical variations over distances comparable with the mushy zone thickness and with the ingot radius existed, samples at the axis of the ingot, at mid-radius, and at the outside diameter were cut. Five chemistries per 21 x 21 mm^2 sample were determined by electron probe analysis. The results indicate that, within a sample, the chemical variations were small with the exception of the freckled area and of the element aluminum. For the latter, variations of the order of 0.5% were observed. The average composition did not change as the ingot grew, except for aluminum; over the duration of the increase in melt rate shown in Figure 2, the aluminum decreased by 0.5%. The variation of composition with radial position indicates that cobalt is enriched at the axis, while titanium, aluminum, and molybdenum are depleted. Dendrite arm spacing measurements were, on the average, 80 μm at the outside diameter, 100 μm at the center, and 120 μm at mid-radius. For steady state velocities ranging from 0.85×10^{-4} to 1.27×10^{-4} ms^{-1}, these dendrite arm spacings correspond to the mushy zone thicknesses of 30 to 46 mm at the outside diameter, 91 to 137 mm at mid-radius, and 55 to 83 mm at the axis.

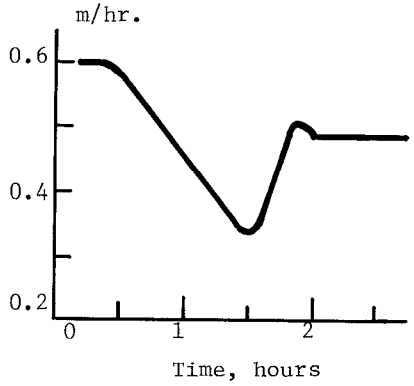

Figure 2: Variation of ingot growth rate in an experimental Waspaloy ingot.

The heat transfer model was used to predict the variation of pool depth during the transient in the melt rate. The predicted liquidus depth matched very closely the pools delineated with tungsten powder (8). The mushy zone depths calculated with the heat transfer model were lower than those calculated from dendrite arm spacing measurements.

At present, the multicomponent macrosegregation model is

not coupled with the heat transfer model and it applies to cases of steady ingot growth. Nevertheless, to see if the correct trend would be predicted, it was used for this transient melt rate case. An average isotherm velocity of 10^{-4} ms^{-1} was calculated with the heat transfer model and was used as a steady growth velocity in the macrosegregation model. The partition ratios for the solutes were estimated from binary diagrams and from spot chemical analyses taken on an as-cast sample. The partition ratios that were used are:

Titanium:	0.80
Aluminum:	0.80
Molybdenum:	0.90
Cobalt:	1.10
Chromium:	1.00
Carbon:	0.25

The permeability was taken to be 6.10^{-5} mm^2 and the liquid metal viscosity 0.003 Pa•s. These values were held constant. The pool shape used in the calculation is shown in Figure 3.

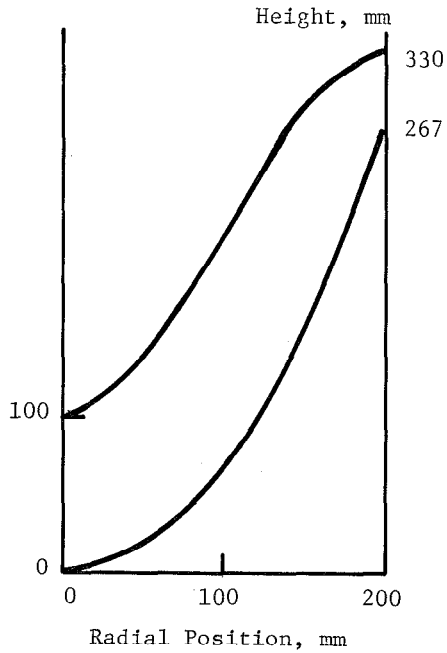

Figure 3: Solidus and liquidus profiles that were assumed in the macrosegregation calculation.

For simplicity, the temperature was assumed to vary linearly with the z direction within the mushy zone. The macrosegregation predicted for the steady growth case is shown in Figures 4a through 4d, together with the measured average compositions corresponding to three radial positions; the averaging is done over the duration of the transient. It is seen that the steady state segregation model predicts correctly the observed trend; the magnitude of the observed segregation is, however, much larger than expected for the solutes aluminum and molybdenum.

DISCUSSION

The work presented in this paper represents a step forward in achieving a mathematical description of the macrosegregation behavior of electroslag remelted superalloys and tool steels.

In the results presented here, the absolute degree of macrosegregation is not correctly predicted for each element. The calculated trend, however, agrees with the experimental observations. Several simplifying assumptions must be pointed out: (a) the formation of a single solid phase down to an assumed invariant eutectic temperature, thus neglecting the formation of the primary carbide (Ti,Mo)C and that of a eutectic of varying compositions; (b) the estimation of the partitioning coefficients from binary phase diagrams and from a limited examination of microsegregation; (c) the estimation of densities, sometimes based on extrapolations and the assumption of ideal mixing; (d) the use of a steady state model to predict macrosegregation during transient; and (e) the assumption that the permeability K varies as the square of the volume fraction of liquid for the entire mushy zone and the assumption that the proportionality factor γ in:

$$K = \gamma g_L^2 \tag{7}$$

is a constant. The literature indicates that Equation 7 has been well established only for $g_L \leq 0.35$ and that the factor γ depends on the dendrite arm spacing (16,17,18). The effect of the convective flow in the liquid pool above the liquidus has been neglected; Ridder's work indicates this is a valid assumption in a first approximate treatment (19). The tungsten powder doping has been assumed to have no effect; a possibility for the decrease in aluminum content over the period of transient is that it reacted with oxygen contamination

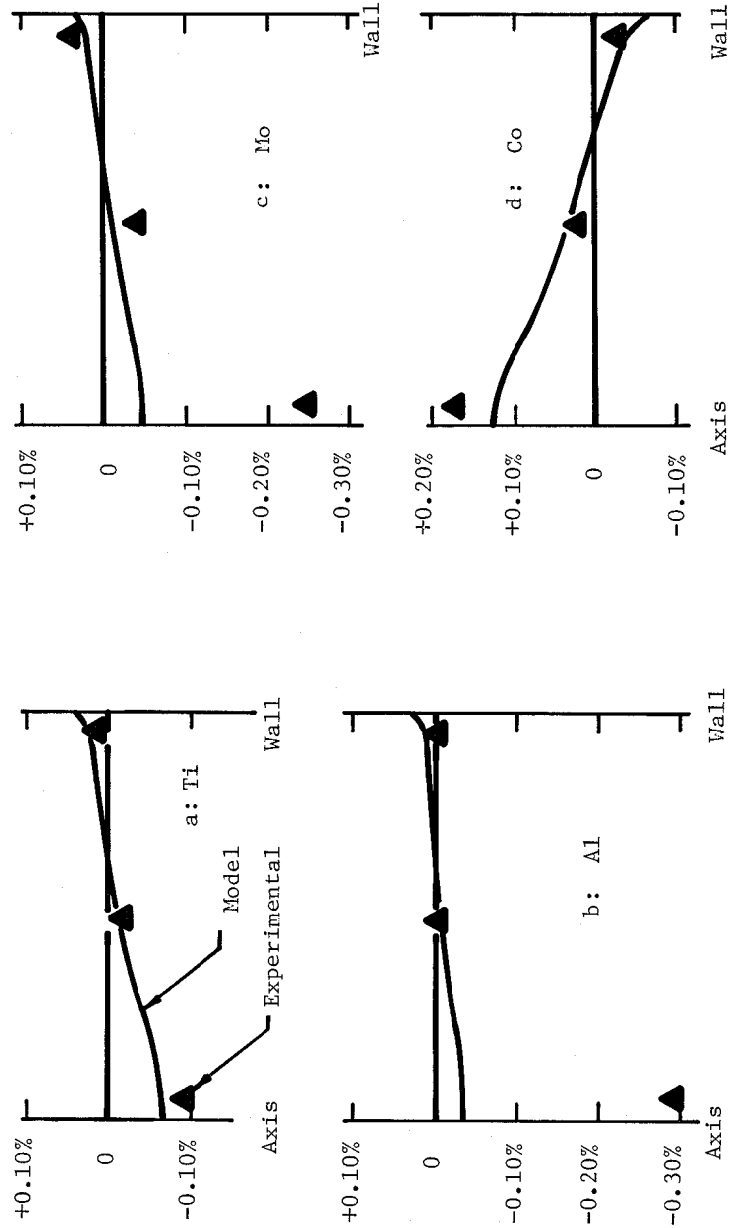

Figure 4: Difference between local ingot composition and average composition as function of radial position.

of the tungsten powder. It is intended to improve the present model by eliminating these simplifying assumptions.

ACKNOWLEDGEMENTS

The authors wish to thank the National Science Foundation (front Number DMR07819699) for its support during this investigation. They also wish to thank Dr. R. Mehrabian of the National Bureau of Standards and Mr. S. D. Ridder of the University of Illinois for their valuable suggestions and comments.

REFERENCES

(1) J. Kreyenberg and K. Schwerdtfeger, "Stirring Velocities Temperature Field in the Slag During Electroslag Remelting," Arch. Eisenh., Vol. 50, 1979, p. 1.

(2) J. Szekely and M. Choudhary, "The Modeling of Pool Profiles, Temperatures, and Fluid Flow Fields in ESR Systems," Proc. of the 6th International Vacuum Metallurgy Conference, April 23-27, 1979, San Diego, California.

(3) M. C. Flemings and G. E. Nereo, "Macrosegregation, Part I," Trans. TMS-AIME, Vol. 239, 1967, p. 1449.

(4) M. C. Flemings, R. Mehrabian, and G. E. Nereo, "Macrosegregation, Part II," Trans. TMS-AIME, Vol. 242, 1968, p. 41.

(5) M. C. Flemings and G. E. Nereo, "Macrosegregation, Part III," Trans. TMS-AIME, Vol. 242, 1968, p. 50.

(6) R. Mehrabian, M. Keane, and M. C. Flemings, "Interdendritic Fluid Flow and Macrosegregation; Influence of Gravity," Met. Trans., Vol. 1, 1970, p. 1209.

(7) A. S. Ballantyne and A. Mitchell, "Modeling of Ingot Thermal Fields in Consumable Electrode Remelting Process," Ironmaking and Steelmaking, No. 4, 1977, p. 222.

(8) C. L. Jeanfils, J. H. Chen, and H. J. Klein, "Temperature Distribution in an Electroslag Remelted Ingot During Transient Conditions," Proc. of the 6th International Vacuum Metallurgy Conference, April 23-27, 1979, San Diego, California.

(9) S. D. Ridder, F. C. Reyes, S. Chakravorty, R. Mehrabian,

J. D. Nauman, J. H. Chen, and H. J. Klein, "Steady State Segregation and Heat Flow in ESR," Met. Trans., Vol. 9B, 1978, p. 415.

(10) T. Fujii, D. R. Poirier, and M. C. Flemings, "Macrosegregation in a Multicomponent Low Alloy Steel," Met. Trans. B, Vol. 10B, 1979, p. 331.

(11) R. Mehrabian and M. C. Flemings, "Macrosegregation in Ternary Alloys," Met. Trans., Vol. 1, 1970, p. 455.

(12) L. D. Lucas, "Liquid Density Measurements," Physicochemical Measurements in Metals Research, Vol. 1V, Part 2, R. A. Rapp, ed.; Intersc. Publ., New York, 1970.

(13) A. Goldsmith et al, eds., Thermophysical Properties of Solid Materials, Vol. 1, McMillan Co., New York, 1969.

(14) Y. S. Touloukian et al, eds., Thermophysical Properties of Matter, Vol. 12: Thermal Expansion-Metallic Elements and Alloys, Plenum Publ. Co., New York, 1975.

(15) M. C. Flemings, "Principles of Control of Soundness and Homogeneity of Large Ingots," Scand. J1. Metallurgy, Vol. 5, 1976, p. 1.

(16) T. S. Piwonka and M. C. Flemings, "Pore Formation in Solidification," Trans. TMS-AIME, Vol. 236, 1966, p. 1157.

(17) D. Apelian, M. C. Flemings, and R. Mehrabian, "Specific Permeability of Partially Solidified Dendritic Networks of Al-Si Alloys," Met. Trans., Vol. 5, 1974, p. 2533.

(18) N. Streat and F. Weinberg, "Interdendritic Fluid Flow in a Lead-Tin Alloy," Met. Trans., Vol. 7B, 1976, p. 417.

(19) S. D. Ridder, Ph.D. Thesis, University of Illinois (1980).